

Article

The Ecological Healthcare Benefits and Influences of Plant Communities in Urban Wetland Parks

Huijun Feng ¹, Jing An ^{1,*}, Haoyun Wang ², Xiongyi Miao ^{1,3,*}, Guangbing Yang ¹, Hongbo Feng ⁴, Yuxiang Wu ¹ and Xuyang Ma ¹

¹ Geography & Environmental Science College, Guizhou Normal University, Guiyang 550025, China; 19306517761@163.com (H.F.); ygbyln@163.com (G.Y.); 15285260829@163.com (Y.W.); m18708569554@163.com (X.M.)

² China College of Forestry, Guizhou University, Guiyang 550025, China; wanghy@gzu.edu.cn

³ Key Laboratory of Karst Dynamics, MNR&GZAR, Institute of Karst Geology, CAGS, Guilin 541004, China

⁴ Lucheng District State Forestry Farm, Changzhi 047500, China; 13835505425@163.com

* Correspondence: anjingsavage@163.com (J.A.); miaoxy88@126.com (X.M.)

Abstract: Plant communities in urban wetland parks (UWP) have significant eco-healthcare benefits in terms of regulating the climate and improving the human living environment. However, factors influencing the regulation of eco-healthcare benefits are unclear. Taking Huaxi Ten Mile Beach National Urban Wetland Park as an example, the urban wetland park comprehensive healthcare index (UPCHI) was constructed based on an outdoor survey and indoor analysis to evaluate the UWP's eco-healthcare benefits. Pathway analysis was used to investigate how climatic, geographic, and plant factors interact to affect the UPCHI. The results show that, over the whole year, tree–shrub–herb showed the best performance in terms of reducing PM_{2.5}, PM₁₀, and noise, as well as raising negative air ion concentrations; however, human comfort performed the worst. The UPCHI was generally beyond level III (0.49–0.58) in the spring and summer, indicating that there are eco-healthcare benefits. Overall, the deciduous tree–shrub–herb community had the highest annual mean UPCHI, and more than half of the plant communities' eco-healthcare benefits were class II, which is very beneficial for eco-healthcare. The main direct factors on UPCHI were illumination intensity (0.68) and tree height (0.90), while canopy height (0.64–0.59) and tree crown radius/canopy height (0.72–0.14) directly or indirectly influenced UPCHI. The distance from the edge of the mountain (−0.39–−0.322) had a direct negative, but minor, effect on UPCHI. This study will assist residents with selecting suitable times and places for wetland recreation and healthcare activities, and it offers a valuable reference for the future planning and design of UWP plant communities.

Keywords: ecological healthcare benefits; urban wetland parks; plant factor; geographical factors; climatic factor



Citation: Feng, H.; An, J.; Wang, H.; Miao, X.; Yang, G.; Feng, H.; Wu, Y.; Ma, X. The Ecological Healthcare Benefits and Influences of Plant Communities in Urban Wetland Parks. *Forests* **2023**, *14*, 2257. <https://doi.org/10.3390/f14112257>

Academic Editors: Anna Maria Palsdottir, Patrik Grahn and Jonathan Stoltz

Received: 27 October 2023

Revised: 12 November 2023

Accepted: 14 November 2023

Published: 16 November 2023



Copyright: © 2023 by the authors. Licensee MDPI, Basel, Switzerland. This article is an open access article distributed under the terms and conditions of the Creative Commons Attribution (CC BY) license (<https://creativecommons.org/licenses/by/4.0/>).

1. Introduction

Rapid urban development has wreaked havoc on the worldwide ecological environment, giving rise to ecological and environmental problems such as urban heat islands and soil and air pollution, in addition to threatening human physical and mental health [1]. With the impact of ecological problems on health and the economy, the awareness of healthcare is gradually increasing and gaining widespread attention [2,3]. According to data from the World Health Statistics 2023 report, the proportion of Chinese urban and rural households that spend more than 10% of their total income and expenditures on healthcare is 24.3%, which is significantly higher than the global rate of 13.5%. Wetlands are land regions covered by water, which feature transitional ecosystems between terrestrial and aquatic environments [4,5]. Due to the constant nourishment from water, the richness and diversity of species are commonly high in wetlands. Wetlands, as one of the three major ecosystems, can not only act as shelter for many organisms, but also mitigate floods and

storms, purify water, and even regulate the climate [6–8], all of which suggest a vital role of wetlands in environmental balance. However, due to increased urbanization, natural wetlands are rapidly shrinking in size, with around 50% of the world's wetlands disappearing since 1900 at a 3.7 times faster rate [9–11]. This heavily degrades the ecological function of natural wetlands and aggravates environmental and climatic disorder, particularly in urban cities [12]. Therefore, artificial wetlands have been proposed as a substitution for natural wetlands for the purpose of mitigating the environmental and climatic disorders in urban cities [13]. As a critical type of artificial wetland, urban wetland parks are rapidly expanding along with the development of green cities. Based on previous studies, more than 800 national wetland parks have been built in China [14], the area of which has reached 3.6 million hectares in total [15]. China is considered to be the country in which the most wetland parks have been constructed. Given the core value of parks for public recreation, the roles of wetland parks should not be limited to ecological balance, but could also extend to tourism and recreation, particularly health tourism. With the significant demand for leisure and tourism, the well-being of urban wetland parks for public health needs to be evaluated, which will not only contribute to the urban ecology but also be conducive to shaping a livable and recreational city.

Urban wetland parks are of great value in terms of increasing public health. Firstly, the humidity from urban wetland parks could partially mediate the heat being released from urban areas, and then decrease the urban heat island effect [13,16,17]. Thus, the construction of urban wetland parks would improve the temperature to a comfortable level and lower energy consumption in urban areas [15,18]. Secondly, wetland plants usually have a thinner wax covering on the surface of their leaves, which is mainly due to the long-term growth in high-humidity environments. They effectively absorb the atmospheric particulate matter and then act as a natural filter to decrease these atmospheric particulate matters [19,20]. Thus, urban wetland parks would minimize the health risks of atmospheric particulate matters, particularly in industrial areas of urban cities. In addition, adequate humidity and vegetation in urban wetland parks could also produce more negative air ions and degrade the noise level more significantly in urban areas. Despite the well-being of the previously listed urban wetland parks, their effectiveness was not stable, particularly with the environment fluctuating. For example, transpiration and shading of vegetation not only impacted the microclimate but also the suspension of particle matter, while photosynthesis and tip discharge on plant leaves also influenced the production and emission of negative air ions [21]. In addition, the distance from pollution sources and roads also significantly altered the particle matter content [22], and the sizes of waterways and their distance from water sources were associated with changes in the human comfort THI [23] and air particulate matters [24]. Given that the environmental variations have rarely been incorporated into the assessment of ecological healthcare benefits of urban wetland parks, it will be indispensable to detail the connections between environmental fluctuations and the well-being of urban wetland parks. This will be beneficial for area planning in urban cities.

Ecological healthcare benefits have been proposed to gauge the health of green land, which includes forests, parks, and recreational land, with multiple health indicators [3,25]. Ecological healthcare benefits refer to the various types of direct beneficial effects of vegetation on human physical and mental health, and consist of a combination of healthcare indicators, including negative air ions (NAI), ambient particulate matter, THI, and noise. With principal component analysis (PCA) and weight analysis (WA), the environmental benefits of plant communities and their connections with healthcare have been assessed [3,26]. However, changes in healthcare indicators are also related to climate, vegetation, and geographic factors. The effects of these factors are complex and variable, and the traditional linear regression models have significant limitations in terms of analyzing or predicting them, particularly the non-linear responses of some variables and the interaction between dependent variables. Thus, according to structural equation modeling (SEM), the developed path analysis (PA) is a conceptual framework based on regression modeling, extended to integrate the consideration

of direct and indirect effects [27]. Despite the valuation system of ecological healthcare benefits being well established and widely applied for the ecological healthcare of forest parks and urban parks, the valuation system of ecological healthcare benefits has rarely been employed in ecological healthcare assessments of urban wetland parks.

The Huaxi Ten Mile Beach National Urban Wetland Park (HBUWP) is the first 4A-grade national urban wetland park in Guizhou Province, China, and was built along the upstream section of the Nanming River in Guiyang City. The gorgeous scenery of HBUWP, including rich vegetation and beautiful river banks, made HBUWP a famous spot for sightseeing and relaxation. Despite HBUWP having already been attractive to local residents and tourists, its healthcare status still remains undetermined. Currently, various roads, buildings, and industrial parks are being constructed nearby due to rapid urbanization, which inevitably raises on the issue of degrading the living quality of local residents and the suitability for leisure tourism. Hence, this study analyzes the following questions for this purpose: (1) Exploring whether Huaxi Ten Mile Beach National Urban Wetland Park have ecological healthcare benefits? (2) What are the regional and temporal variations in the ecological health benefits of urban wetland parks? (3) How do vegetation characteristics, geographic location, and climatic factors affect eco-health benefits in urban wetland parks? The investigation of healthcare benefits in urban wetland parks would not only support the construction of urban wetland parks, but also optimize the community structure of plants in urban wetland parks, all of which would support the creation of ecological cities.

2. Materials and Methods

2.1. Study Area

Huaxi Ten Mile Beach National Urban Wetland Park (HBUWP) stretches from Niujiào Island to Huaxi Bridge, with a total area of 4.6 km², the longitude and latitude of which are 106°40'23.4"–106°40'59.129" E, 26°26'20.9"–26°27'55.463" N, respectively. HBUWP belongs to a humid subtropical climate; the annual mean temperature commonly stays at 14.9 °C, which suggests a pleasant climate without harsh winters or blistering summers. The park has a significant abundance of botanical resources, with 495 species of vascular plants and 51 species of higher plants, accounting for 27.6% of the total number of higher wetland plants in Guizhou Province (185 species). Wetland landscape resources are dominated by artificial forests with good growth conditions, and the main tree species include *Metasequoia glyptostroboides*, *Prunus persica*, *ginkgo biloba*, *Osmanthus fragrans*, *Magnolia grandiflora*, and *Cerasus serrulata*, among others. The main shrub species are *Photinia × fraseri*, *Pittosporum tobira*, *Nandina domestica*, *Fatsia japonica*, etc. The main herb plants are *Lolium perenne*, *Poa pratensis*, *Iris tectorum*, *Gladiolus gandavensis*, *Trifolium repens*, and *Euryops pectinatus*, among others.

2.2. Sample Plot Setting and Plant Community Survey

The ten typical plant communities include evergreen tree (A1), evergreen tree–shrub (herb) (A2), evergreen tree–shrub–herb (A3), deciduous tree (B1), deciduous tree–shrub (herb) (B2), deciduous tree–shrub–herb (B3), waterside trees (C1), waterside tree–shrub (herb) (C2), waterside tree–shrub–herb (C3), and lawn (L). In addition, two unforested control groups, located at the park's entrance (CK1) and in the hydrostatic region (CK2), were selected for this study. Sampling in triplicate was established for each type of sample in each site to elevate the robustness and dependability of this research. The investigation of plant communities was conducted using the Swedish quadrant approach, as described by Niu et al. [28]. We set up 20 m × 20 m tree, shrub, and grass samples in the four corners of the tree samples, respectively; the area of each shrub sample was 5 m × 5 m and that of the herb sample was 1 m × 1 m. This was based on the empirical value of the minimum area of an evergreen deciduous broadleaf mixed forest. Geographic information and plant information were recorded during the sampling process. The geographic information was included as follows: distance from the edge of the lake (HL), distance from the edge of

the mountain (ML), and distance from the edge of the park (BL). Plant information was included as follows: arbor diameter at breast height (DBH), tree height (TH), tree crown size (TCS), tree crown radius (TCR), canopy height (CH), tree crown radius/canopy height (TCR/CH), number of trees (TN), tree canopy volume (TCV), shrub height (SH), shrub volume (SV), herb volume (HV), number of plant community stratification (NPCS), and tree density (TM). Geographic information was recorded using a GPS receiver (positioning accuracy: 1 m); DBH, TH, TCS, TCR, CH, and SH were determined using a tree measuring instrument (measuring range: 5–254 cm; accuracy: 0.1°); and TCV, SV, and HV were estimated for each plant, a process which was adopted from Zhou Jianhua et al.'s three-dimensional greenness model [29]. Figure 1 and Table 1 indicate the location of the study region as well as the fundamental conditions of the sample plots.

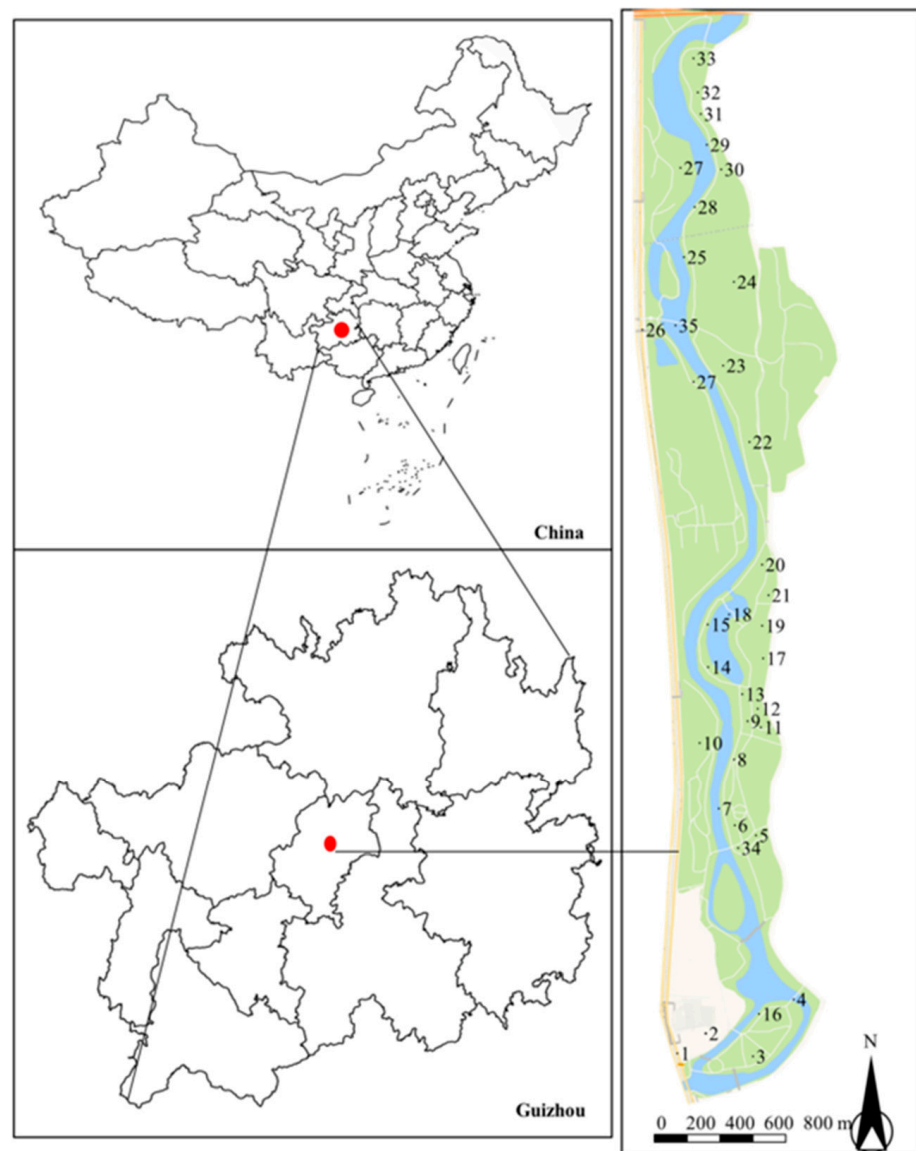


Figure 1. Schematic map of the location of the sample point in Huaxi Ten Mile Beach National Urban Wetland Park.

Table 1. Plot overview of Huaxi Ten Mile Beach National Urban Wetland Park.

| Plot No | Main Species of Plot | Tree Species | Shrub Species | Herbaceous Species | Greenbelt Types | Monitoring Points (Figure 1) |
|---------|--|--|---|---|--------------------------------|------------------------------|
| CK1 | Entrance of the park hydrostatic region | | | | control sites | 1, 2, 26 |
| CK2 | | | | | control sites | 4, 18, 35 |
| L | <i>Poa annua</i> | | | <i>Lolium perenne</i> , <i>Poa annua</i> | lawn | 22, 23, 30 |
| A1 | <i>Cinnamomum camphora</i> | <i>Cinnamomum camphora</i> | | | evergreen tree | 3, 27, 32 |
| A2 | <i>Cinnamomum camphora</i> - <i>Nandina domestica</i> | <i>Cinnamomum camphora</i> | <i>Hibiscus syriacus</i> ., <i>Photinia serratifolia</i> , <i>Nandina domestica</i> | | evergreen tree–shrub (herb) | 6, 21, 34 |
| A3 | <i>Osmanthus fragrans</i> - <i>Photinia serratifolia</i> - <i>Pleioblastus amarus</i> | <i>Osmanthus fragrans</i> 'Latifolius', <i>Cinnamomum camphora</i> , <i>Magnolia Grandiflora</i> | <i>Nandina domestica</i> - <i>Photinia serratifolia</i> | <i>Iris tectorum</i> , <i>Cortaderia selloana</i> , <i>Pleioblastus amarus</i> | evergreen tree–shrub–herb | 5, 11, 33 |
| B1 | <i>Metasequoia glyptostroboides</i> | <i>Metasequoia glyptostroboides</i> | | | deciduous tree | 10, 17, 19 |
| B2 | <i>Metasequoia glyptostroboides</i> - <i>Hosta plantaginea</i> | <i>Metasequoia glyptostroboides</i> | | <i>Hosta plantaginea</i> | deciduous tree–shrub (herb) | 12, 13, 20 |
| B3 | <i>Pterocarya stenoptera</i> - <i>Nandina domestica</i> - <i>Hosta plantaginea</i> | <i>Pterocarya stenoptera</i> | <i>Nandina domestica</i> , <i>Photinia serratifolia</i> | <i>Hosta plantaginea</i> , <i>Cortaderia selloana</i> , <i>Dianthus chinensis</i> | deciduous tree–shrub–herb | 8, 9, 31 |
| C1 | <i>Salix babylonica</i> , <i>Prunus persica</i> | <i>Salix babylonica</i> , <i>Prunus persica</i> | | | water's edge trees | 7, 28, 29 |
| C2 | <i>Metasequoia glyptostroboides</i> - <i>Iris pseudacorus</i> | <i>Metasequoia glyptostroboides</i> | | <i>Iris pseudacorus</i> , <i>Reineckia carnea</i> | water's edge tree–shrub (herb) | 15, 25, 27 |
| C3 | <i>Metasequoia glyptostroboides</i> - <i>Hibiscus mutabilis</i> - <i>Phragmites australis</i> | <i>Metasequoia glyptostroboides</i> , <i>Prunus serrulata</i> <i>var. lannesiana</i> | <i>Hibiscus mutabilis</i> , <i>Boehmeria penduliflora</i> | <i>Phragmites australis</i> | water's edge tree–shrub–herb | 14, 16, 24 |

2.3. Monitoring of Healthcare Indicators

From March 2021 to January 2022, three consecutive sunny days with wind speed < 2 m/s were selected in each season, and five environmental and climatic indicators were collected. The five healthcare indicators included human comfort (THI), ambient particulate matter concentration (PM_{2.5}, PM₁₀), negative air ion concentration (NAI), and noise. The three climatic indicators were illumination intensity, temperature, and humidity. The negative air ion concentration was measured with an air ion counter (measurement range: 1–5 × 10⁷ ion·cm⁻³; mobility: ≥ 0.4 cm²·v⁻¹·S⁻¹; measurement accuracy: 1 ion·cm⁻³). PM_{2.5} and PM₁₀ were determined via a handheld airborne particulate counter (measuring range 0–2 × 10³ µg·m⁻³, resolution 1 µg·m⁻³). Temperature and humidity were measured using a handheld thermohydrometer (temperature measuring range: –20–50 °C; accuracy: ±0.6 °C; humidity measuring range: 0%–100%; accuracy: 2%–3% RH). Noise was tested using a digital noise decibel meter (measuring range: 30–130 dBA; accuracy: ±1.5 dB),

and the illumination intensity was measured via a recording type of illuminance meter (measuring range: $0.01-9.99 \times 10^5$ Lux; accuracy: $\pm 3\%$). All instruments were installed at a height of 1.5 m above the ground. The measurements were performed at consistent intervals of 2 h, starting at 8:00 and ending at 18:00, during the spring, summer, and autumn seasons. In the winter, the measurements were taken from 8:00 to 16:00. Measurements were taken using five points in four directions (east, south, west, and north) at and near the center point, and the average value was taken as the measurement value. In this study, the thermal humidity index (THI) was chosen as the calculation standard for human comfort (Table 2) [30].

Table 2. THI evaluation standards.

| Evaluation Grade | THI | Body Comfort | Body Feeling |
|------------------|-------------|--------------|---------------------|
| I | ≥ 27.5 | Intense heat | Quite uncomfortable |
| II | 25.5–27.5 | Hot | Not comfortable |
| III | 17.0–25.5 | Warm | Comfortable |
| IV | 14.0–16.9 | Cold | Not comfortable |
| V | < 14.0 | Very cold | Quite uncomfortable |

The thermal humidity index (THI) was calculated as:

$$\text{THI} = T - 0.55(1 - \text{RH})(T - 14.5) \quad (1)$$

where T is the air temperature ($^{\circ}\text{C}$) and RH is the relative humidity (%).

2.4. Multiple Indicators Comprehensive Evaluation Methods

The five healthcare indicators that had previously been assessed were standardized and categorized into positive effect indicators, which indicate that larger values are more favorable for ecological healthcare, and negative effect indicators, which suggest that smaller values are more beneficial for ecological healthcare. NAI in all seasons and THI in spring, autumn, and winter served as positive effect indicators and were standardized using Equation (2). The THI in the summer, as well as the noise, $\text{PM}_{2.5}$, and PM_{10} in all seasons, served as negative effect indicators and were standardized using Equation (3).

Also, a principal component and weighting analysis was conducted using the five healthcare indicators, which were grouped into three principal components as shown in Table 3. The cumulative contribution rate of these three main components was 93.91%, exceeding 80%. This indicates that the chosen components successfully captured and represented the information which the indicators conveyed. The three function formulas were denoted as (4), (5), and (6).

Table 3. Coefficient matrix of principal component scores for environmental indicators.

| Index | Principal Component | | |
|-------------------------------------|---------------------|--------|--------|
| | 1 | 2 | 3 |
| THI (X_1) | −0.008 | 0.688 | 0.519 |
| $\text{PM}_{2.5}$ (X_2) | 0.370 | 0.080 | 0.189 |
| PM_{10} (X_3) | 0.371 | 0.090 | 0.156 |
| NAI (X_4) | −0.174 | −0.348 | 0.938 |
| Noise (X_5) | 0.281 | −0.419 | 0.141 |
| Cumulative contribution to variance | 52.141 | 77.634 | 93.907 |

The specific formula for the urban wetland park comprehensive healthcare index (UPCHI) was denoted as (7). In the Origin2022 software, UPCHI evaluation levels were determined using the Ward and Euclidean distance method [3] to analyze the UPCHI

values systematically. These values were adjusted based on Zhu Shuxin's research findings and practical requirements. The UPCHI values were divided into six levels ranked from high to low, each representing a distinct intensity of comprehensive healthcare care benefits (Table 4).

Table 4. UPCHI evaluation standards.

| Evaluation Grade | Index Range | Level | Effect on Health |
|------------------|-------------------|-----------|-----------------------|
| I | UPCHI \geq 0.57 | Fabulous | Extremely beneficial |
| II | 0.57–0.53 | Fabulous | Very beneficial |
| III | 0.53–0.48 | Very good | Beneficial |
| IV | 0.48–0.25 | Good | Normal |
| V | 0.25–0.04 | General | Unfavorable |
| VI | UPCHI < 0.04 | Very bad | Extremely unfavorable |

The formula was as follows:

$$X'_{ij} = (X_{ij} - \min X_{ij}) / (\max X_{ij} - \min X_{ij}) \quad (2)$$

$$X'_{ij} = (\max X_{ij} - X_{ij}) / (\max X_{ij} - \min X_{ij}) \quad (3)$$

$$F1 = -0.008X_1 + 0.370X_2 + 0.371X_3 - 0.174X_4 + 0.281X_5 \quad (4)$$

$$F2 = 0.688X_1 + 0.080X_2 + 0.090X_3 - 0.348X_4 - 0.419X_5 \quad (5)$$

$$F3 = 0.519X_1 + 0.189X_2 + 0.156X_3 + 0.938X_4 + 0.141X_5 \quad (6)$$

$$\text{UPCHI} = 0.56F1 + 0.27F2 + 0.17F3 \quad (7)$$

where X is the original value of each indicator; X' is the standardized value; i is the i th monitoring indicator $i = 1, 2, \dots, n$; j represents the different plant communities, $j = 1, 2, \dots, m$; $F1, F2, F3$ are the scores of the main components; X_1, X_2, X_3, X_4 and X_5 are the normalized values of THI, $\text{PM}_{2.5}$, PM_{10} , NAI and noise, respectively.

2.5. Data Analysis

The data were stored and organized using Microsoft Excel. Statistical analyses such as descriptive statistical analysis (the mean and standard deviation), ANOVA, multiple comparisons, principal component analysis, regression analysis, and cluster analysis were performed using SPSS (version 20). Visual representations such as boxplots, correlation analyses, and bar charts were generated using Origin (version 22) and GraphPad Prism (version 8.0.1). AMOS (version 28) was used for the construction and analysis of the path model, and model fit tests were performed using a goodness of fit index (GFI) of 0.9, root mean square error of approximation (RMSEA) of less than 0.1 [31], and a ratio of chi-square degree of freedom (χ^2/df) values of less than 3 [32].

3. Results

3.1. Human Comfort Dynamic

In the spring, the plant community was classified as class III. The level of physical comfort was determined to be "comfortable" (Table 1 and Figure 2). The THI value of C1 was found to be the highest (23.04), while the value of A2 was the lowest (19.64) and the values of A2 and A3 were significantly lower than those of the rest of the plant community ($p < 0.05$). In the summer, the overall comfort level was usually low, which suggests a physically uncomfortable environment for the public. The lowest THI value was C3, which reached 26.01, while the highest THI value (27.02) was determined to be L. The THI values

for A1, A2, A3, and C3 were considerably lower than those of the control group ($p < 0.05$). In autumn, the lowest THI value was observed for the A3 (13.34), while the highest THI value was found for the B3 (15.30). The fluctuations of THI in winter (0–1.45) were relatively small, but their values were significantly lower than those in other seasons, which suggests a physically uncomfortable environment.

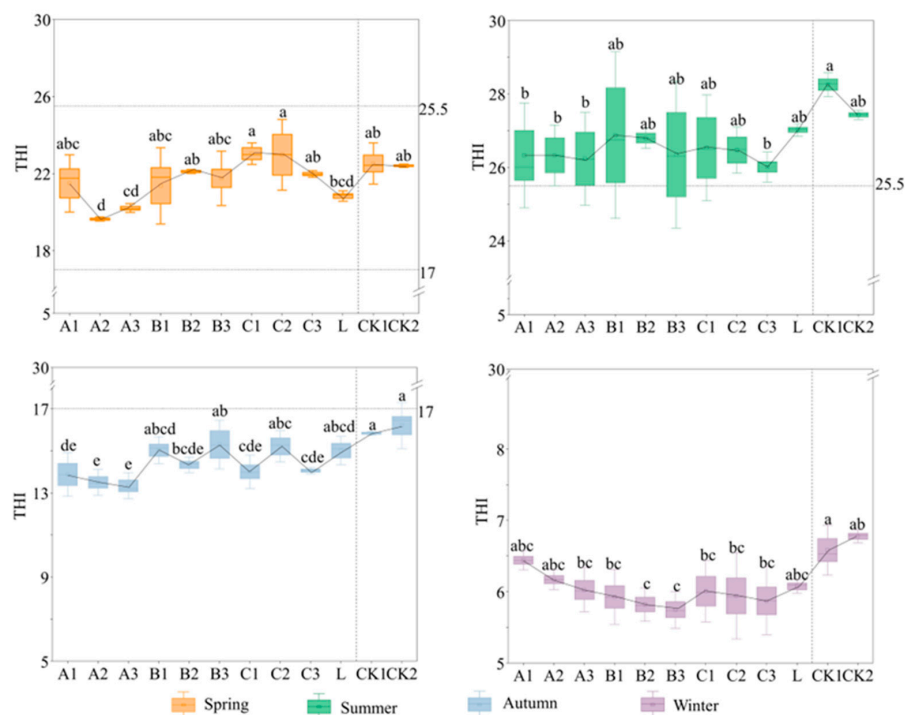


Figure 2. THI change chart. A1: evergreen tree; A2: evergreen tree–shrub (herb); A3: evergreen tree–shrub–herb; B1: deciduous tree; B2: deciduous tree–shrub (herb); B3: deciduous tree–shrub–herb; C1: waterside trees; C2: waterside tree–shrub (herb); C3: waterside tree–shrub–herb; L: lawn; CK1: the park entrance; CK2: the hydrostatic region. The two dashed lines from 17 to 25.5 represent a comfort level of III, i.e., “warm and comfortable.” Different lowercase letters indicate significant differences between different community structures at the same time ($p < 0.05$).

3.2. $PM_{2.5}$, PM_{10} Dynamics

The variation in $PM_{2.5}$ concentration in each plant community was found to be significant in different seasons (Figure 3a). It is worth noting that the concentrations of $PM_{2.5}$ were at their lowest in the B2 for spring and summer, while the highest $PM_{2.5}$ concentration was found in the A1. Compared to the control group, the $PM_{2.5}$ concentration in each plant community commonly expressed lower percentages of 0.18%–33.03% for spring and 2.31%–35.49% for summer, respectively. Except for A1, all plant communities were substantially different from CK1 ($p < 0.05$). The $PM_{2.5}$ concentration in A3 was lowest in the autumn and winter, while the concentration of $PM_{2.5}$ in B1 was highest. Compared to the control group, the $PM_{2.5}$ concentration in each plant community commonly expressed lower percentages of 4.8%–33.67% for autumn and –1.17%–6.08% for winter. Furthermore, it was observed that the evergreen community types differed significantly from the control group throughout the autumn season ($p < 0.05$). The variation in PM_{10} concentration in the plant community was determined not to be the same as that of $PM_{2.5}$ concentration (Figure 3b). Compared to the CK1, each plant community experienced a reduction, which ranged from 5.21% to 34.90%. In the summer, the variations in PM_{10} concentration were determined between B2 and B3, but the variations in the rest of the plant community were considered not to be significant ($p > 0.05$). Compared to the control group, the concentration of PM_{10} in these communities exhibited a reduction, which ranged from 10.52% to 27.35%. In autumn, the PM_{10} concentration in A3 was the lowest, but was highest

in C3. Compared to the control group, all plant communities decreased in a range from 0% to 23.52%. In the winter, the PM_{10} concentration in B3 was the lowest ($76.25 \mu\text{g}\cdot\text{m}^{-3}$), while it was highest in A1, which showed a decreased percentage of -1.97% – 4.15% compared with the control group. The lower PM_{10} concentration in winter may be attributed to the constant rain prior to PM_{10} concentration monitoring. Finally, the most striking result was that the ambient particulate matter concentrations were lower throughout the year for L and CK2. Particularly in autumn, the PM_{10} concentration in the L was only higher than that in evergreen community types.

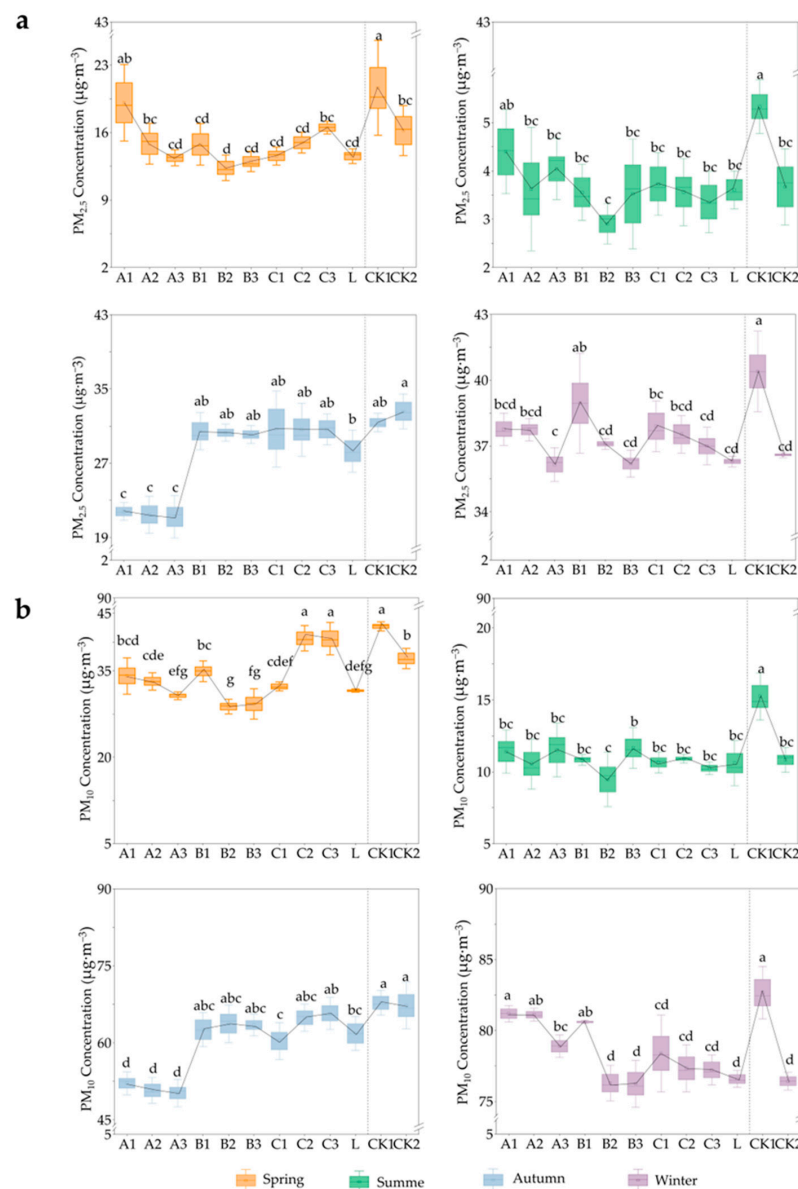


Figure 3. $PM_{2.5}$, PM_{10} concentration change chart. (a) is a graph of daily changes in $PM_{2.5}$, (b) is a graph of daily changes in PM_{10} . A1: evergreen tree; A2: evergreen tree–shrub (herb); A3: evergreen tree–shrub–herb; B1: deciduous tree; B2: deciduous tree–shrub (herb); B3: deciduous tree–shrub–herb; C1: waterside trees; C2: waterside tree–shrub (herb); C3: waterside tree–shrub–herb; L: lawn; CK1: the park entrance; CK2: the hydrostatic region. Different lowercase letters indicate significant differences between different community structures at the same time ($p < 0.05$).

3.3. Negative Air Ion Concentration Dynamics

The data in Figure 4 demonstrate the variations in NAI concentration among different plant communities in different seasons. The concentration of NAI was lowest in L regardless

of the season. The C3 structural NAI concentration was highest in the spring, which was a significantly different result from the control group ($p < 0.05$). The NAI concentrations in A3 were at the maximum in summer, autumn, and winter: 1147.88 ions·cm⁻³, 578.64 ions·cm⁻³, and 418.19 ions·cm⁻³, respectively. These concentrations were substantially different from those of the control group ($p < 0.05$). Furthermore, the varying community configurations were 1.32–3.04, 1.24–2.66, 0.96–2.48, and 1.12–2.39 times higher than those of the control group in different seasons, respectively. In general, the NAI concentrations were higher in tree structures than in tree–shrub (herb) structures during the summer and autumn.

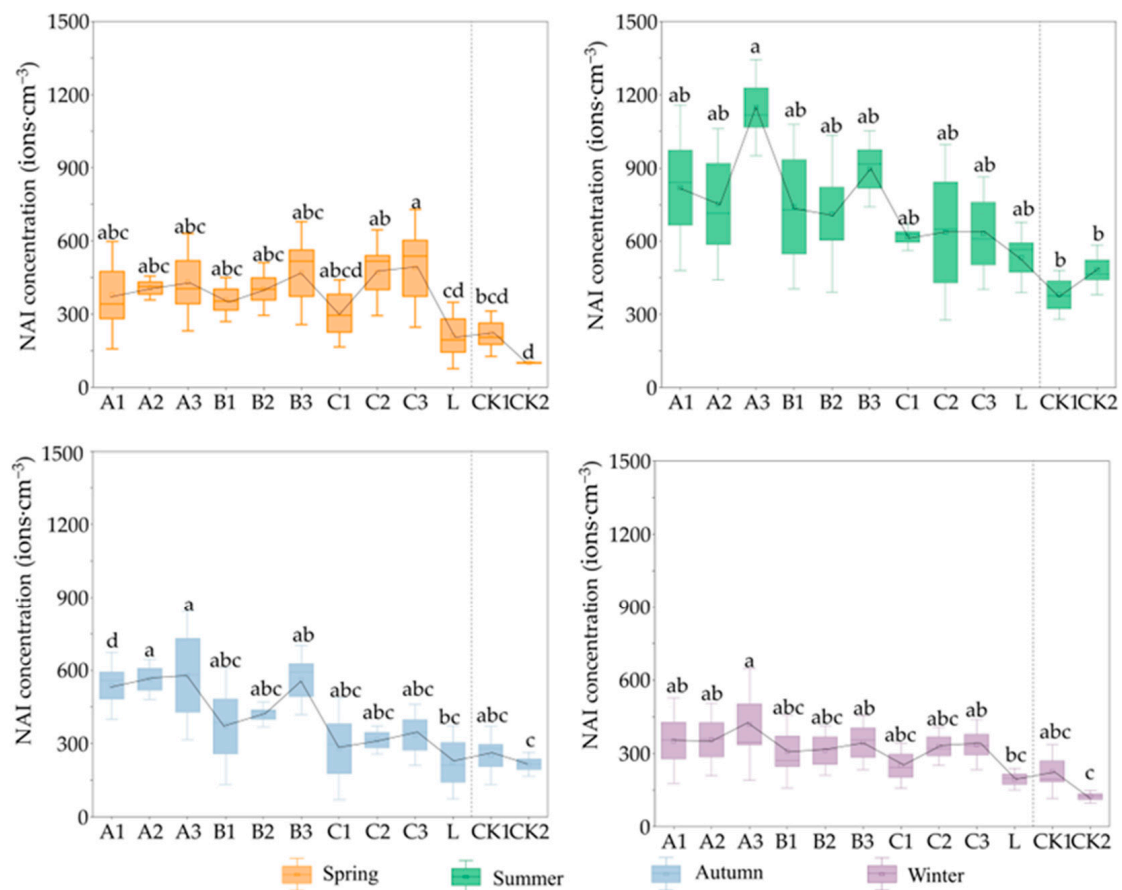


Figure 4. NAI concentration change chart. A1: evergreen tree; A2: evergreen tree–shrub (herb); A3: evergreen tree–shrub–herb; B1: deciduous tree; B2: deciduous tree–shrub (herb); B3: deciduous tree–shrub–herb; C1: waterside trees; C2: waterside tree–shrub (herb); C3: waterside tree–shrub–herb; L: lawn; CK1: the park entrance; CK2: the hydrostatic region. Different lowercase letters indicate significant differences between different community structures at the same time ($p < 0.05$).

3.4. Noise Dynamics

The results in Figure 5 demonstrate the noise trend in different plant communities between seasons. The variation in the noise level in the plant community was confirmed to be significant in each season ($p < 0.05$). In the spring, the B1 exhibited the lowest noise level, at 51.93 dB(A), while the A1 had the highest noise level, at 57.35 dB(A). Compared to the noise at the park's entrance, each plant community experienced a reduction in noise level, which ranged from 11.28% to 19.67%. In the summer, the A2 had the lowest noise level of 55.42 dB(A), while the B2 had the highest noise level of 62.28 dB(A); each plant community experienced a noise reduction of 0.79%–11.72% compared to the noise of the control group. The noise level in A3 reached 51.51 dB(A) for autumn and 47.78 dB(A) for winter. Compared to the control group, each plant community experienced drops of 13.01% to 23.03% and of 1.08% to 13.8%.

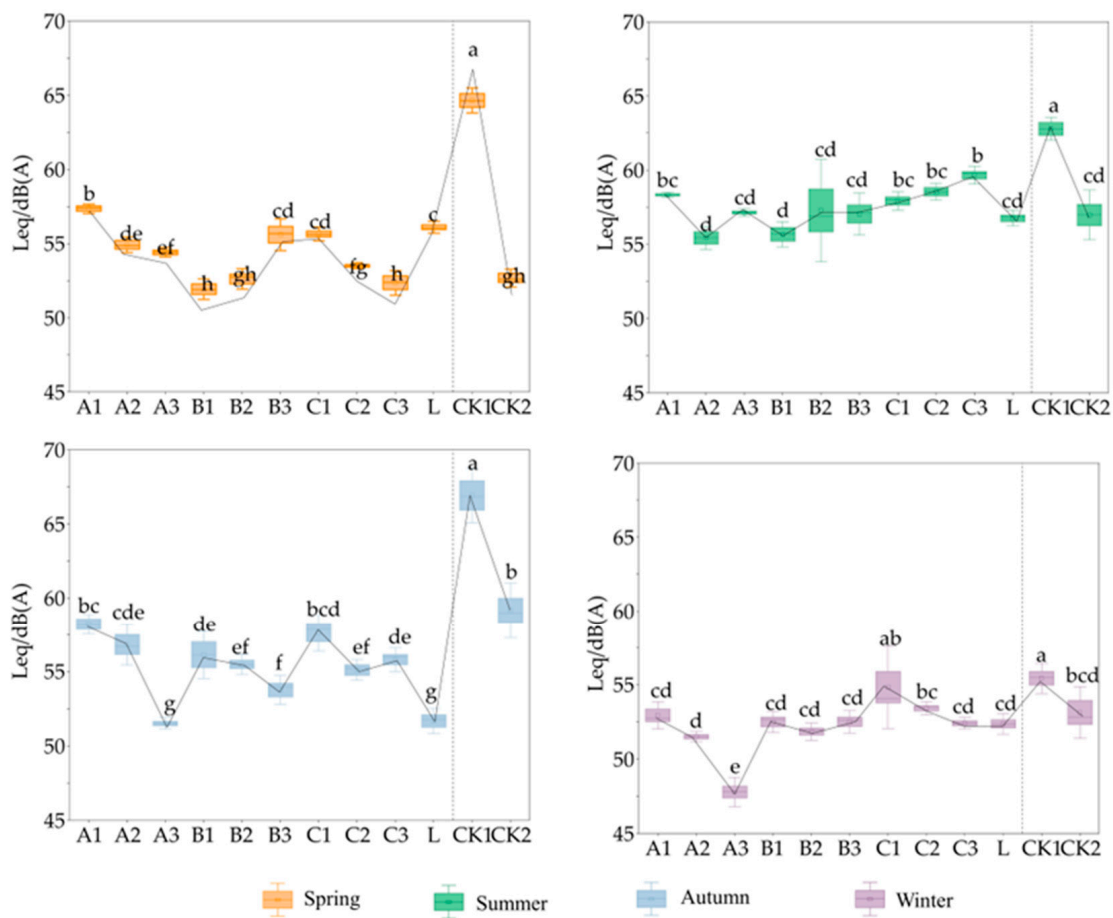


Figure 5. Noise change chart. A1: evergreen tree; A2: evergreen tree–shrub (herb); A3: evergreen tree–shrub–herb; B1: deciduous tree; B2: deciduous tree–shrub (herb); B3: deciduous tree–shrub–herb; C1: waterside trees; C2: waterside tree–shrub (herb); C3: waterside tree–shrub–herb; L: Lawn; CK1: the park entrance; CK2: the hydrostatic region. Different lowercase letters indicate significant differences between different community structures at the same time ($p < 0.05$).

3.5. The Ecological Healthcare Benefits Dynamics

Based on the above environmental variables, a system of eco-healthcare benefit indicators was developed to gauge the eco-healthcare benefits of each plant community (Figure 6, Table 3). The results suggest that the UPCHI of the plant community reached III levels and higher in the spring, which should be considered to be beneficial for healthcare. Among them, the UPCHI of B3 was determined to be the highest, while that of C2 was treated as the lowest. In the summer, except for L, all plant communities reached II level, suggesting them to be “Very beneficial” for healthcare. The B3 was still the highest UPCHI value (0.55), and the lowest UPCHI was found for L. In autumn, except for C2 and C3, the other UPCHI of the plant community only reached the IV level, which suggests a “normal” healthcare benefit. The A3 had the highest UPCHI value (0.37), while the C2 had the lowest UPCHI value (0.24). In the winter, the whole community had values between the levels of V and VI, suggesting an extremely unfavorable environment for healthcare.

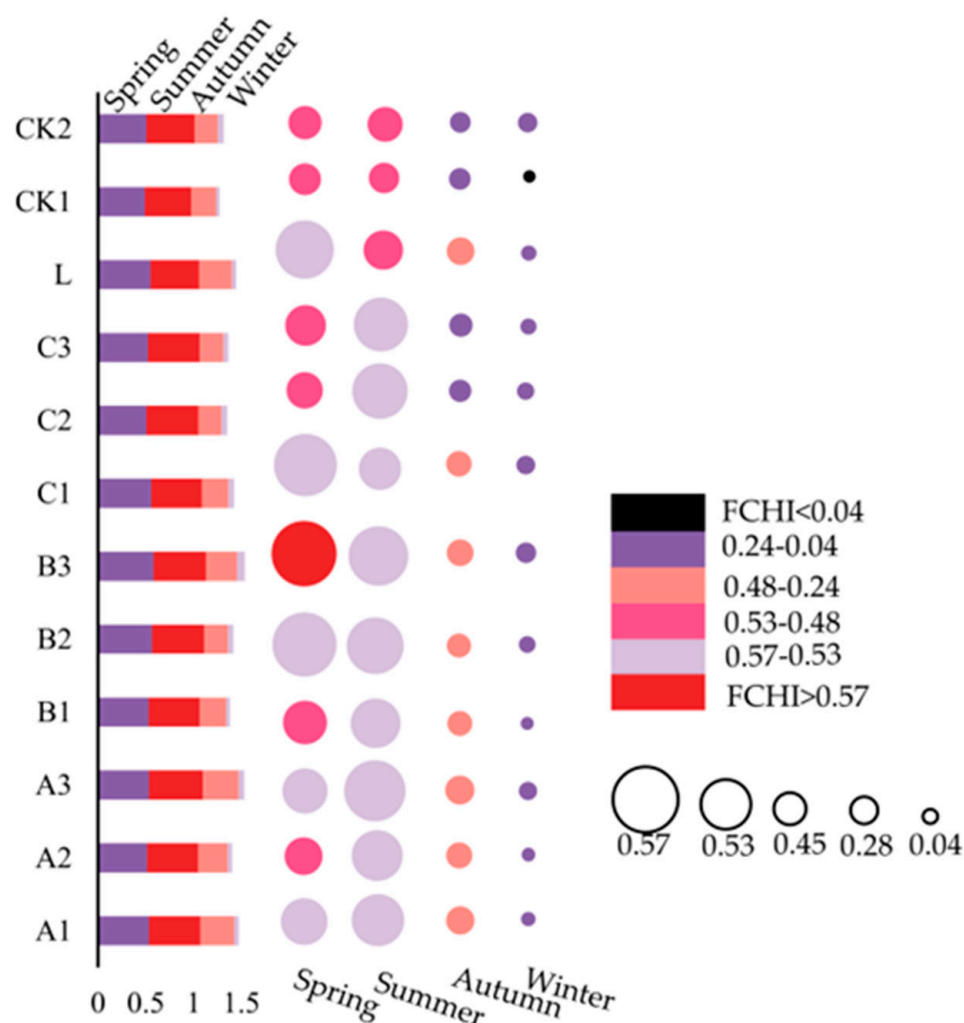


Figure 6. UPCHI change chart. UPCHI: urban wetland park comprehensive healthcare index; A1: evergreen tree; A2: evergreen tree–shrub (herb); A3: evergreen tree–shrub–herb; B1: deciduous tree; B2: deciduous tree–shrub (herb); B3: deciduous tree–shrub–herb; C1: waterside trees; C2: waterside tree–shrub (herb); C3: waterside tree–shrub–herb; L: lawn; CK1: the park entrance; CK2: the hydrostatic region.

In the spring and winter, UPCHI decreased according to the community types as follows (Figure 7): deciduous community types (0.55, 0.06) > waterside community types (0.53, 0.54) > evergreen community types (0.52, 0.05). The difference between deciduous community types and evergreen community types was significant in the spring ($p < 0.05$). In the summer, the UPCHI decreased according to the community types as follows: deciduous community type (0.54) > evergreen community type (0.53) > waterside community type (0.53). In autumn, the order was as follows: evergreen community type (0.35) > deciduous community type (0.38) > waterside community type (0.25), and the difference between the UPCHI values of evergreen community types was significantly different from those of deciduous and waterside community types ($p < 0.001$). In terms of the community structure, in the spring and autumn the UPCHI decreased as follows: tree–shrub–herb structure (0.54, 0.31) > tree structure (0.53, 0.30) > tree–shrub (herb) structure (0.52, 0.26). The difference between the autumn evergreen community types and deciduous and waterside community types was significant ($p < 0.01$). The order was tree–shrub–herb structure (0.54, 0.06) > tree–shrub (herb) structure (0.54, 0.05) > tree structure (0.53, 0.04) in the summer and winter.

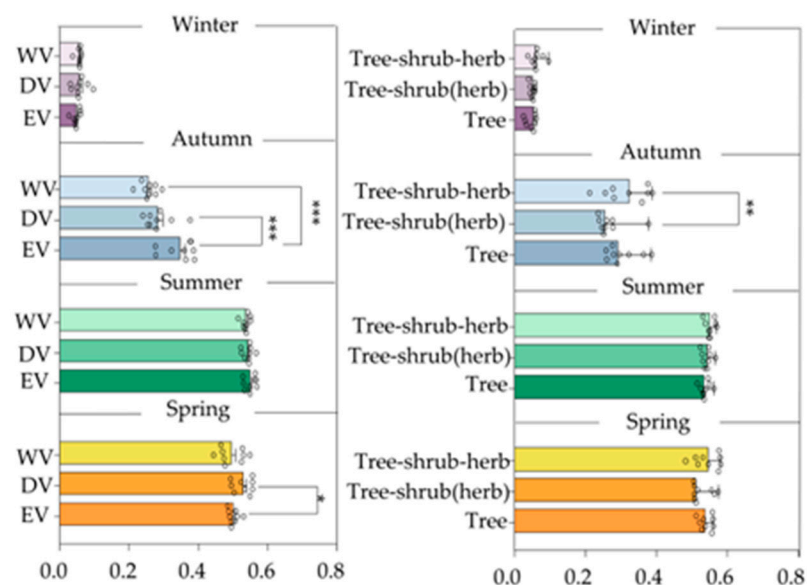


Figure 7. Plant community type (left) and plant community structure (right) for the UPCHI change chart. UPCHI: urban wetland park comprehensive healthcare index; EV: plant evergreen community type; DV: plant deciduous community type; WV: plant waterside community type. Significance levels are as follows: *** $p < 0.001$, ** $p < 0.01$, * $p < 0.05$.

3.6. Effect of Multi-Factors on UPCHI

The correlations between plant, geographical, and climatic factors and UPCHI were analyzed for all seasons, and the results are given in Figure 8. In the spring, the correlation of UPCHI was confirmed to be significant with DBH, CH, TCV, ML, and illumination intensity. These correlations were positive with DBH, CH, and TCV, but negative with ML and illumination intensity. In the summer, UPCHI was significantly correlated with TH, TCR/CH, TCR, DBH, CH, CS, TCV, BL, illumination intensity, ML, and temperature. The correlation coefficients of DBH, CH, CS, TCV, and BL were positive, while the correlation coefficients of illumination intensity, ML, and temperature were negative. In autumn, the correlations between air humidity, TN, TCV, HV, and UPCHI were found to be significant. These correlations were positive for air humidity, TN, and TCV, but negative for HV. In winter, the correlations between CS, DBH, TCR, SH, and TM all had positive correlation coefficients. In addition, a significant negative correlation between UPCHI and TM was also observed.

3.7. Multi-Factor Pass Analysis of UPCHI

Given the higher UPCHI, spring and summer were chosen for the path analysis (Figures 6 and 8). The following two well-fitting models were developed through continuous evaluation and correction of the relationships between variables (Figure 9). In the spring, CH, DBH, and illumination intensity (positive), as well as ML (negative), showed significant direct influences on UPCHI, and TCR/CH showed a significant negative indirect influence through illumination intensity, with path coefficients of 0.638, 0.385, 0.683, -0.390 , and -0.226 , respectively. In the summer, CS, TCR/CH, TH, ML, HL, air temperature, and TCR showed a direct influence on UPCHI, with path coefficients of 0.413, 0.722, 0.903, -0.322 , -0.278 , 0.201, and -0.869 , respectively. Surprisingly, the TCV was shown not to have a direct influence. Furthermore, BL and illumination intensity demonstrated an indirect influence on UPCHI via numerous pathways. Illumination intensity and air temperature were the most significant, with path coefficients of -0.196 and 0.713. It is important to note that DBH has no influence on UPCHI. Finally, the summer plant component had a critical influence on illumination intensity.

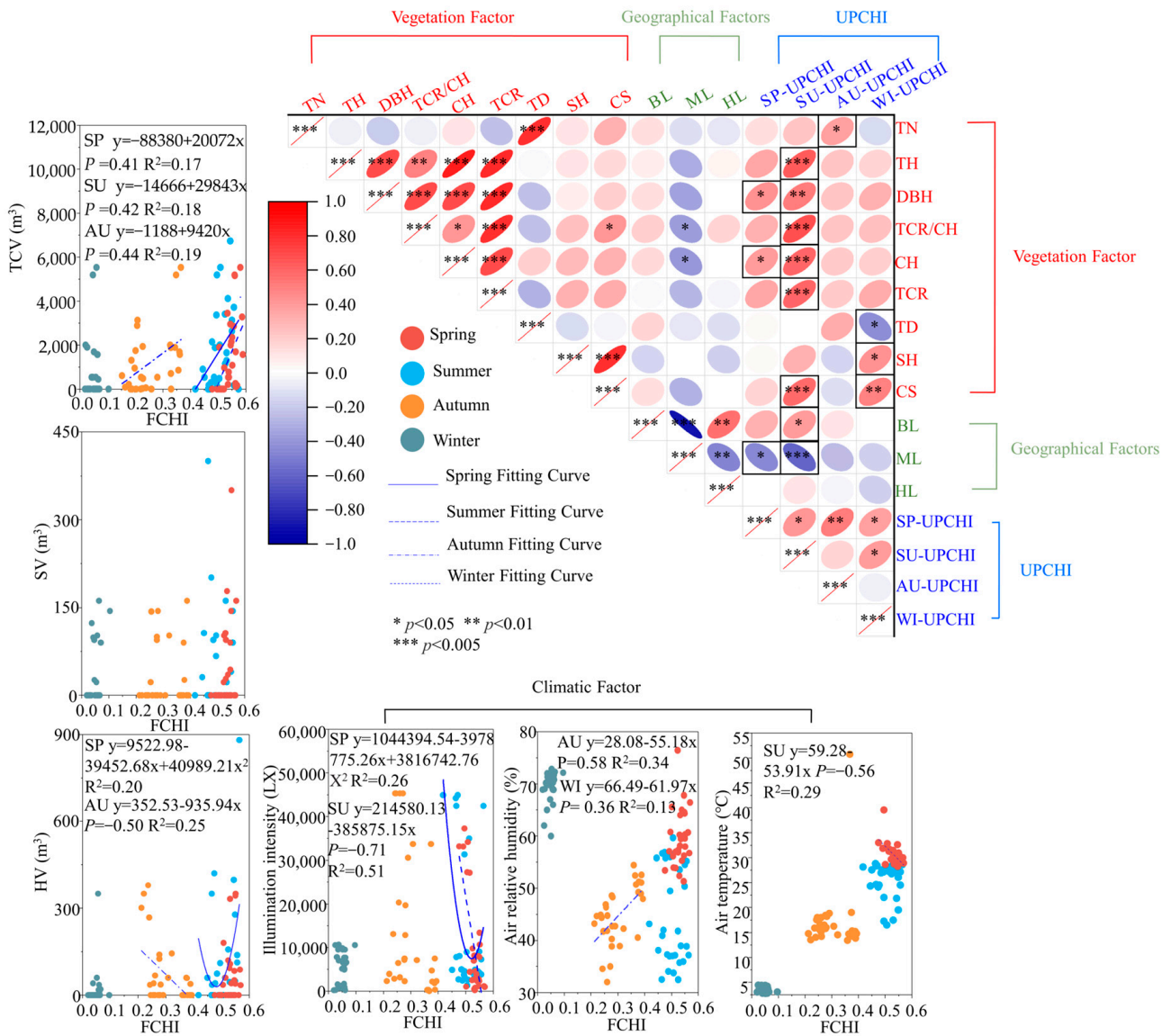


Figure 8. UPCHI correlation analysis chart. UPCHI: urban wetland park comprehensive healthcare index; SP: spring; SU: summer; AU: autumn; WI: winter; TN: number of trees; TH: tree height; DBH: diameter at breast height; TCR/CH: tree crown radius/canopy height; CH: canopy height; TCR: tree crown radius; SH: shrub height; CS: the plant community stratification; TD: tree density; TCV: tree volume; SV: shrub volume; HV: herb volume; BL: distance from the park edge; ML: distance from the mountain; HL: distance from the river edge.

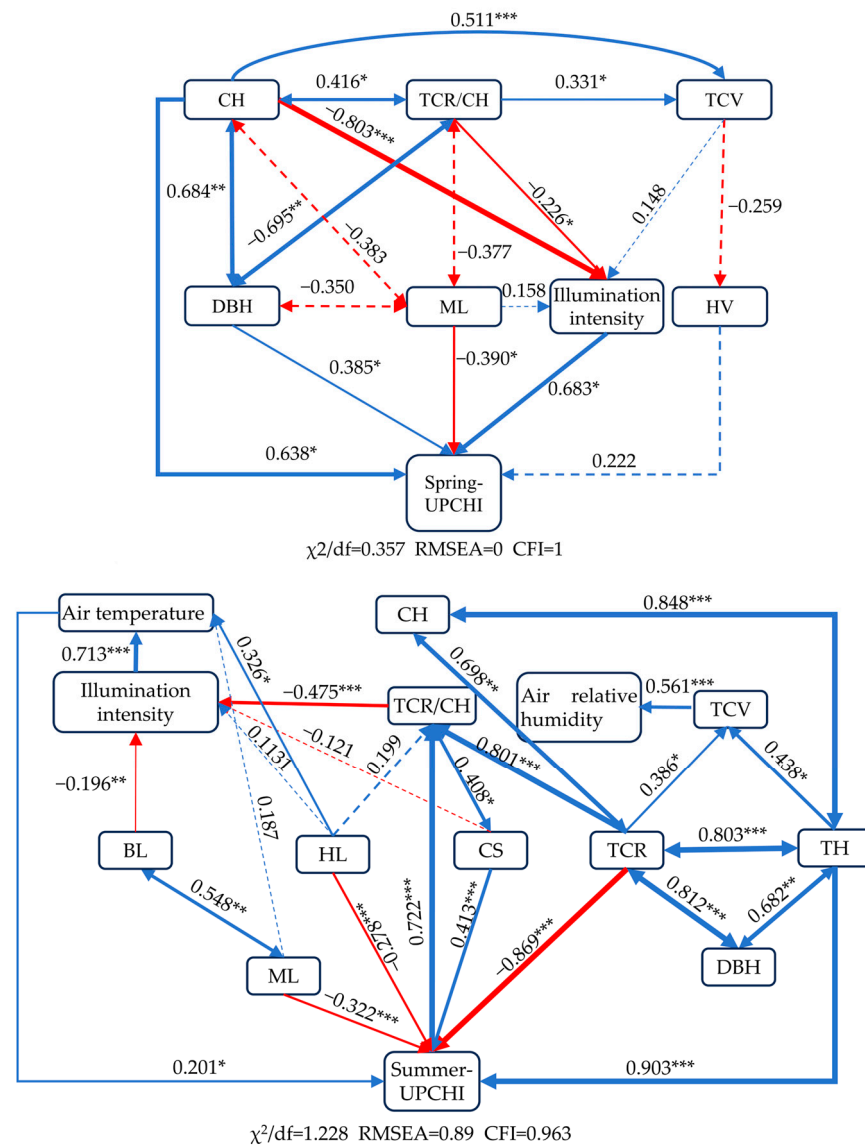


Figure 9. UPCHI path analysis chart. UPCHI: urban wetland park comprehensive healthcare index; TH: tree height; DBH: diameter at breast height; TCR/CH: tree crown radius/canopy height; CH: canopy height; TCR: tree crown radius; CS: the number of plant community stratifications; TCV: tree volume; HV: herb volume; BL: distance from the park edge; ML: distance from the mountain; HL: distance from the river edge. Dashed lines indicate no significance and solid lines indicate significance. The thickness of the line indicates the importance of the influencing factors. The blue line indicates a positive influence relationship and the red line indicates a negative influence relationship. The value next to each arrow indicates the normalized path factor. One-way arrows indicate influence relationships, and two-way arrows indicate correlation relationships. Significance levels are as follows: *** $p < 0.001$, ** $p < 0.01$, * $p < 0.05$.

4. Discussion

4.1. Changes in Ecological Health Benefits

Air particulate matter, negative air ions, human comfort, and noise are all components of the UPCHI. Summer had the greatest UPCHI, and principal component analysis suggests that airborne particulate matter contributed the most to the UPCHI index, followed by negative air ions and human comfort. Although higher temperatures and humidity reduce human comfort in the summer, the high-humidity environment increases the aggregated and weight of suspended airborne particulate matter, which is susceptible to dry and

wet deposition [33], and the high temperatures contribute to airborne particulate matter diffusion, resulting in the lowest airborne particulate matter concentrations occurring in the summer. At the same time, the low concentration of airborne particulate matter reduces binding to negatively charged NAI in the air and, thus, reduces NAI loss. However, in terms of plant communities, the plant community with the best UPCHI across all seasons did not occur in the summer, but in the deciduous tree–shrub–herb structure in the spring, which could be due to a combination of a suitable temperature and humidity environment in the spring and the vigorous growth of spring-sprouting leaves of deciduous plants, which would produce more negative air ions and a higher level of comfort.

UPCHI performed the best in terms of plant community type and structure, with a deciduous community type and tree–shrub–herb structure. This may be due to the large number of *M. glyptostroboides*, *T. distichum*, *G. biloba*, *P. Cerasifera Ehrhar*, and *f. atropurpurea* plants in the deciduous plant community, which have smaller and denser leaves and rough foliage that capture more PM [34,35]. In addition, deciduous plants have higher water transport efficiency and photosynthetic capacity [36], and can produce NAI. Furthermore, noise does not show regularity due to the mobility of tourists and the influence of the surrounding traffic and factories. The comfort results which we achieved were influenced by the fact that the measurement stations in this study were placed in areas with flat terrain and little variation in elevation, resulting in a more uniform microclimate. As a result, deciduous community types have superior ecological health. Because the tree–shrub–herb structure is characterized by shrubs and herbaceous plants beneath the tree canopy, the space is fully utilized, and the amount of spatial three-dimensional greenery per unit of green space area is relatively large. This type of structure can deposit more vertical spatial PM and produce more NAI than single- and double-story structures.

Eco-health benefits are influenced by a combination of factors, but traditional correlation analysis only revealed the correlation and magnitude of each relevant factor regarding eco-health benefits. However, the relationships between eco-health benefits and each influential factor were complex. Constructing a pathway analysis model would clearly show the magnitude and relative importance of the correlation of each relevant factor, indicate the causal relationships between the roles of the variables [37–39], and reveal the relationships between the variables in a more profound way.

4.2. Influence of Plant Factors on the UPCHI

Vegetation provides ecological benefits such as climate regulation, air purification, boosting NAI concentrations, and lowering noise and dust. The influences of plant parameters on UPCHI vary with the changing season. According to correlation and pathway analyses, CH, TCR/CH, and TH were considered as the critical vegetative elements that can impact UPCHI, while TV did not have an influential role in UPCHI. This demonstrated that tree crown geometry had the greatest influence on UPCHI. In the spring, CH had the highest direct route coefficient with UPCHI, indicating that CH was the most closely associated with UPCHI and an essential factor in improving UPCHI. This could be because plant communities with high CH in the spring have large under-canopy spaces, which increases the capacity for heat convection between the interior and exterior of the plant community [40]. This results in increased temperature and wind speed within the community, increased air friction producing NAI and PM diffusion [41–43], and proper ventilation contributing to thermal comfort. The direct path coefficients of TH and TCR/CH on UPCHI were larger in the summer. Higher TH and TCR/CH values often corresponded to taller trees, larger crowns, and lower sub-canopy heights, which naturally expressed more leaves, larger-sized crowns, and greater degrees of canopying [44]. A canopy blocks solar radiation and reduces heat, and a greater evapotranspiration capacity removes latent heat [45,46], resulting in a cooling effect that improves human comfort. Previous studies have proven that tall trees with large canopies have superior photosynthesis and transpiration; thus, they are more likely to produce large amounts of water vapor, which is conducive to reducing the ambient

particulate matter [22], adjusting the local microclimate [44], degrading the noise level [47], and producing NAI [48].

4.3. Influence of Climatic Factors on the UPCHI

In the spring, LX directly affected UPCHI, the direct path coefficient of which was similar to that of CH. This indicates that the increase in these two factors can significantly improve the UPCHI values of different plant communities while keeping other factors unchanged. Therefore, LX should be a crucial factor in the spring to obtain a better UPCHI. LX had a greater impact on UPCHI, which could be because an increase in illumination intensity promotes the photolysis of organic carbon in PM, lowering PM concentrations [49]. Also, an increase in illumination intensity raises the near-surface temperature, enhancing atmospheric convection and promoting the upward movement and diffusion of PM. At the same time, rising temperatures cause losses of ammonium nitrate and other volatile PM ingredients PM [50,51], lowering PM concentrations. A rising temperature enhances the acceleration of the thermal motion of atoms or molecules [52], increasing the possibility of collisions and ionization between them, which can result in more NAIs. Illumination intensity can also be employed to boost NAI production by encouraging plant photosynthesis, which emits oxygen and negative ions into the atmosphere, and oxygen molecules have a high ability to absorb electrons. However, contrary to our prediction, the summer UPCHI did not significantly affect the relationship with temperature or illumination intensity, which may be because the present study was conducted during clear and windless weather. The UPCHI values may have been less influenced by the background general climate and more significantly by the microclimate. However, the extremely high temperatures and light in summer, as well as the lush vegetation and high stand depression, resulted in few differences between the microclimates of each plant community.

4.4. Influence of Geography Factors on the UPCHI

Geographic factors influence pollution conditions and moisture changes in the plant community, and cause UPCHI to vary among plant communities. This study found that the distance from the mountain (ML) had some impact on the UPCHI factors of the plant community. On the one hand, this could be because the research area was in the shape of a belt closer to the ML and farther away from the BL, while outside the park were roads, universities, and factories. As a result, people, automobiles, and manufacturing operations contribute to air pollution by increasing the concentration of airborne particulates and the loss of NAI. On the other hand, the mountain woodland region may encompass a broad area and have a substantial impact on localized air particle matter and NAI.

5. Conclusions

The ultimate purpose of this research was to quantify the combined eco-healthcare benefits of plant communities and determine the major elements influencing eco-healthcare benefits. Firstly, each plant community had a significantly higher UPCHI value than the unforested control throughout the year, with the best UPCHI values in spring and summer. This was shown to have an effect on human health. Among them, the *Pterocarya stenoptera*–*Nandina domestica*–*Hosta plantaginea* deciduous tree–shrub–herb category, i.e., the B3 structure, had the highest UPCHI, followed by *Osmanthus fragrans*–*Photinia serratifolia*–*Pleioblastus amarus* (A3). Second, the tree height (TH) and tree crown radius/canopy height (TCR/CH) were the primary direct factors influencing UPCHI, while the canopy height (CH) and tree crown radius/canopy height had an indirect impact on UPCHI by decreasing the illumination intensity and increasing the degree of plant community stratification. When compared to vegetative factors, geographic and climatic factors had less significant effects on UPCHI. Overall, the UPCHI of the vegetation community was influenced by the interactions between multiple factors. Therefore, in the future, tourists can travel to areas characterized by a tree–shrub–herb structure in urban wetland parks for healthcare activities in the spring and summer. Furthermore, park planners should

focus on restructuring vegetation communities. In particular, emphasis should be placed on increasing deciduous vegetation and trees with CH, TCR/CH, and TH characteristics; more recreational areas in areas close to mountains would maximize the health benefits of plant communities. This study provides a reference for future studies aiming to optimize the ecological health benefits of urban humidity parks.

Author Contributions: H.F. (Huijun Feng): conceptualization, data curation, formal analysis, methodology, visualization, writing—original draft, writing—review and editing; J.A.: conceptualization, formal analysis, writing—review and editing; H.W.: writing—review and editing; X.M. (Xiongyi Miao): writing—review and editing; G.Y.: writing—review and editing; H.F. (Hongbo Feng): writing—review and editing; Y.W.: writing—review and editing; X.M. (Xuyang Ma): writing—review and editing. All authors have read and agreed to the published version of the manuscript.

Funding: This work was supported in full by grants from the Joint Fund of the National Natural Science Foundation of China and the Karst Science Research Center of Guizhou Province (Grant No. U1812401) and Innovation and the Entrepreneurship Training Plan Project for Provincial College Students of Guizhou Normal University (S202210663061).

Data Availability Statement: The data that support the findings of this study are available from the corresponding author, [J.A.], upon reasonable request.

Conflicts of Interest: The authors declare no conflict of interest.

References

- Liu, L.; Li, J.; Wang, J.; Liu, F.; Cole, J.; Sha, J.; Jiao, Y.; Zhou, J. The establishment of an eco-environmental evaluation model for southwest China and eastern South Africa based on the DPSIR framework. *Ecol. Indic.* **2022**, *145*, 109687. [[CrossRef](#)]
- Liao, L.; Du, M.; Chen, Z. Environmental pollution and socioeconomic health inequality: Evidence from China. *Sustain. Cities Soc.* **2023**, *95*, 104579. [[CrossRef](#)]
- Zhu, S.X.; Hu, F.F.; He, S.Y.; Qiu, Q.S.; Yan, H.; Qian, L.; Ji, Y. Comprehensive Evaluation of Healthcare Benefits of Different Forest Types: A Case Study in Shimen National Forest Park, China. *Forests* **2021**, *12*, 207. [[CrossRef](#)]
- Dou, X.Y.; Guo, H.D.; Zhang, L.; Liang, D.; Zhu, Q.; Liu, X.T.; Zhou, H.; Lv, Z.R.; Liu, Y.M.; Guo, Y.T.; et al. Dynamic landscapes and the influence of human activities in the Yellow River Delta wetland region. *Sci. Total Environ.* **2023**, *899*, 166239. [[CrossRef](#)] [[PubMed](#)]
- Wei, Q.F.; Shao, Y.; Xie, C.; Cui, B.S.; Tian, B.S.; Brisco, B.; Li, K.; Tang, W.J. Number and Nest-Site Selection of Breeding Black-Necked Cranes Over the Past 40 Years in the Longbao Wetland Nature Reserve, Qinghai, China. *Big Earth Data* **2021**, *5*, 217–236. [[CrossRef](#)]
- Pan, M.X.; Hu, T.G.; Zhan, J.Y.; Hao, Y.; Li, X.Q.; Zhang, L.X. Unveiling spatiotemporal dynamics and factors influencing the provision of urban wetland ecosystem services using high-resolution images. *Ecol. Indic.* **2023**, *151*, 110305. [[CrossRef](#)]
- Xu, Y.M.; Xie, Y.J.; Wu, X.D.; Xie, Y.T.; Zhang, T.Y.; Zou, Z.X.; Zhang, R.T.; Zhang, Z.Q. Evaluating temporal-spatial variations of wetland ecosystem service value in China during 1990–2020 from the donor side based on cosmic exergy. *J. Clean. Prod.* **2023**, *414*, 137485. [[CrossRef](#)]
- Zhang, B.; Shi, Y.T.; Liu, J.H.; Xu, J.; Xie, G.D. Economic values and dominant providers of key ecosystem services of wetlands in Beijing, China. *Ecol. Indic.* **2017**, *77*, 48–58. [[CrossRef](#)]
- Davidson, N.C. How much wetland has the world lost? Long-term and recent trends in global wetland area. *Mar. Freshw. Res.* **2014**, *65*, 934. [[CrossRef](#)]
- Zhu, X.L.; Jiao, L.; Wu, X.; Du, D.S.; Wu, J.J.; Zhang, P. Ecosystem health assessment and comparison of natural and constructed wetlands in the arid zone of northwest China. *Ecol. Indic.* **2023**, *154*, 110576. [[CrossRef](#)]
- Mahapatra, A.; Hore, U.; Singh, A.; Kumari, M. The effect of urbanization on the shrinkage of wetlands in the Noida-Greater Noida region and its surrounding sub-urban areas. *Acta Ecol. Sin.* **2023**; *in press*. [[CrossRef](#)]
- Yan, J.; Zhu, J.; Zhao, S.Y.; Su, F.Z. Coastal wetland degradation and ecosystem service value change in the Yellow River Delta, China. *Glob. Ecol. Conserv.* **2023**, *44*, e02501. [[CrossRef](#)]
- Liu, L.; He, H.Y.; Cai, Y.H.; Hang, J.; Liu, J.; Liu, L.; Jiang, P.; He, H. Cooling effects of wetland parks in hot and humid areas based on remote sensing images and local climate zone scheme. *Build. Environ.* **2023**, *243*, 110660. [[CrossRef](#)]
- Zhou, J.B.; Wu, J.; Gong, Y.Z. Valuing wetland ecosystem services based on benefit transfer: A meta-analysis of China wetland studies. *J. Clean. Prod.* **2020**, *276*, 122988. [[CrossRef](#)]
- Ye, Y.; Qiu, H.F. Environmental and social benefits, and their coupling coordination in urban wetland parks. *Urban For. Urban Green.* **2021**, *60*, 127043. [[CrossRef](#)]
- Wu, S.J.; Yang, H.; Luo, P.; Luo, C.; Li, H.L.; Liu, M.; Ruan, Y.; Zhang, S.J.; Xiang, P.; Jia, H.H.; et al. The effects of the cooling efficiency of urban wetlands in an inland megacity: A case study of Chengdu, Southwest China. *Build. Environ.* **2021**, *204*, 108128. [[CrossRef](#)]

17. Şimsek, Ç.K.; Ödul, H. Investigation of the effects of wetlands on micro-climate. *Appl. Geogr.* **2018**, *97*, 48–60. [[CrossRef](#)]
18. Cao, X.; Onishi, A.; Chen, J.; Imura, H. Quantifying the cool island intensity of urban parks using ASTER and IKONOS data. *Landsc. Urban Plan.* **2010**, *96*, 224–231. [[CrossRef](#)]
19. Willis, K.J.; Petroofsky, G. The natural capital of city trees. *Science* **2017**, *356*, 374–376. [[CrossRef](#)]
20. Yan, G.X.; Liu, J.K.; Zhu, L.J.; Zhai, J.X.; Cong, L.; Ma, W.M.; Wang, Y.; Wu, Y.N.; Zhang, Z.M. Effectiveness of wetland plants as biofilters for inhalable particles in an urban park. *J. Clean. Prod.* **2018**, *194*, 435–443. [[CrossRef](#)]
21. Li, A.; Li, Q.L.; Zhou, B.Z.; Ge, X.G.; Cao, Y.H. Temporal Dynamics of Negative Air Ion Concentration and its Relationship with Environmental Factors: Results from Long-Term On-Site Monitoring. *Sci. Total Environ.* **2022**, *832*, 155057. [[CrossRef](#)] [[PubMed](#)]
22. Zhu, C.Y.; Przybysz, A.; Chen, Y.; Guo, H.J.; Chen, Y.Y.; Zeng, Y.Z. Effect of spatial heterogeneity of plant communities on air PM10 and PM2.5 in an urban forest park in Wuhan, China. *Urban For. Urban Green.* **2019**, *46*, 126487. [[CrossRef](#)]
23. Kim, Y.; Yu, S.Y.; Li, D.Y.; Gatson, S.N.; Brown, R.D. Linking landscape spatial heterogeneity to urban heat island and outdoor human thermal comfort in Tokyo: Application of the outdoor thermal comfort index. *Sustain. Cities Soc.* **2022**, *87*, 104262. [[CrossRef](#)]
24. Zhou, X.F.; Zhang, S.; Zhu, D. Impact of Urban Water Networks on Microclimate and PM_{2.5} Distribution in Downtown Areas: A Case Study of Wuhan. *Build. Environ.* **2021**, *203*, 108073. [[CrossRef](#)]
25. Tang, H.X.; Yang, Q.; Jiang, M.Y.; Wang, T.X.; Li, X.; Chen, Q.B.; Luo, Z.H.; Lv, B.Y. Seasonal Variation in the Thermal Environment and Health-Related Factors in Two Clustered Recreational Bamboo Forests. *Forests* **2023**, *14*, 1894. [[CrossRef](#)]
26. Yang, C.; Wang, Y.R.; Tang, Z.Y.; Wang, Q.; Duan, M.J.; Qi, L.H. Ecological health care effects of scenic recreational forests with different community structures: A case study of Beijing Xishan National Forest Park. *Acta Ecol. Sin.* **2022**, *42*, 6499–6513.
27. Sha, Z.P.; Ma, X.; Liu, H.J.; Wang, J.X.; Lv, T.T.; Goulding, K.; Liu, X. Crop-specific ammonia volatilization rates and key influencing factors in the upland of China—A data synthesis. *J. Environ. Manag.* **2023**, *336*, 117676. [[CrossRef](#)] [[PubMed](#)]
28. Niu, X.; Li, Y.; Li, M.N.; Zhang, T.; Meng, H.; Zhang, Z.; Wang, B.; Zhang, W.K. Understanding vegetation structures in green spaces to regulate atmospheric particulate matter and negative air ions. *Atmos. Pollut. Res.* **2022**, *13*, 101534. [[CrossRef](#)]
29. Zhou, J.H.; Sun, T.Z. Remote sensing model study of three-dimensional green biomass and estimation of greening environmental benefits. *Natl. Remote Sens. Bull.* **1995**, *3*, 162–174.
30. Asghari, M.; Ghalhari, G.; Ghanadzadeh, M.; Moradzadeh, R.; Tajik, R.; Samadi, S.; Samadi, S.; Heidari, H. Modeling of thermal discomfort based representative concentration pathways (RCP) scenarios in coming decades using temperature-humidity index (THI) and effective temperature (ET): A case study in a semi-arid climate of Iran. *Air Qual. Atmos. Health* **2023**, *16*, 1195–1205. [[CrossRef](#)]
31. Chen, L.X.; Chen, Z.S.; Jia, G.D.; Zhuo, J.; Zhao, J.C.; Zhang, Z.Q. Influences of forest cover on soil freeze-thaw dynamics and greenhouse gas emissions through the regulation of snow regimes: A comparison study of the farmland and forest plantation. *Sci. Total Environ.* **2020**, *726*, 138403. [[CrossRef](#)]
32. Duan, C.S.; Wu, Z.F.; Liao, H.; Ren, Y. Interaction Processes of Environment and Plant Ecophysiology with BVOC Emissions from Dominant Greening Trees. *Forests* **2023**, *14*, 523. [[CrossRef](#)]
33. Li, J.; Chen, H.B.; Li, Z.Q.; Wang, P.C.; Cribb, M.; Fan, X.H. Low-level temperature inversions and their effect on aerosol condensation nuclei concentrations under different large-scale synoptic circulations. *Adv. Atmos. Sci.* **2015**, *32*, 898–908. [[CrossRef](#)]
34. Przybysz, A.; Nersisyan, G.; Gawroński, S. Removal of particulate matter and trace elements from ambient air by urban greenery in the winter season. *Environ. Sci. Pollut. Res. Int.* **2018**, *26*, 473–482. [[CrossRef](#)] [[PubMed](#)]
35. Baraldi, R.; Neri, L.; Costa, F.; Facin, O.; Rapparini, F.; Carriero, G. Ecophysiological and micromorphological characterization of green roof vegetation for urban mitigation. *Urban For. Urban Green.* **2019**, *37*, 24–32. [[CrossRef](#)]
36. Ni, R.W.; Gan, Y.T.; Yang, G.M.; Huang, L.J.; Liu, X.Z.; Run, S.J. Trade-off characteristics of stomata of subtropical urban vegetation and its relationship with leaf functional traits under heat island effect. *Acta Ecol. Sin.* **2023**, *43*, 5336–5346.
37. Tilahun, T.; Bezie, Y.; Petros, Y.; Dessalegn, Y.; Taye, M. Correlation and path coefficient analysis of green pod yield and yield attributing traits of chili (*Capsicum annum* L.) genotypes in Ethiopia. *All Life* **2022**, *15*, 203–210. [[CrossRef](#)]
38. Gayathri, S.; Lal, G.; Lavanya, G.R.; Maddula, S.R.; Shika, U. Estimation of Correlation and Path Coefficient Analysis for Quantitative Traits in Chickpea (*Cicer arietinum* L.): An Experimental Study. *Int. J. Environ. Clim. Change* **2022**, *12*, 2185–2193. [[CrossRef](#)]
39. Hinson, P.O.; Adams, C.B.; Dong, X.J.; Xue, Q.W.; Thapa, S.; Feng, G.N.; Kimura, E.; Pincha, B.; Somenahally, A.; Somenahally, A.; et al. Path analysis of phenotypic factors associated with grain protein in dryland winter wheat. *J. Crop Improv.* **2022**, *36*, 892–918. [[CrossRef](#)]
40. Liu, H.X.; Wu, J.; Xu, L.J.; Xu, C.Y. Selection of Canopy Structure Index of Urban Forest Associated with Comfort Degree of Microclimate Within the Forest. *Sci. Silvae Sin.* **2020**, *56*, 32–39.
41. Wang, H.; Wang, B.; Niu, X.; Song, Q.F.; Li, M.H.; Luo, Y.Y.; Liang, L.D.; Du, P.C.; Peng, W.L. Study on the change of negative air ion concentration and its influencing factors at different spatio-temporal scales. *Glob. Ecol. Conserv.* **2020**, *23*, e01008. [[CrossRef](#)]
42. Abdi, B.; Hami, A.; Zarehaghi, D. Impact of small-scale tree planting patterns on outdoor cooling and thermal comfort. *Sustain. Cities Soc.* **2020**, *56*, 102085. [[CrossRef](#)]
43. Sodoudi, S.; Zhang, H.W.; Chi, X.L.; Müller, F.; Li, H.D. The influence of spatial configuration of green areas on microclimate and thermal comfort. *Urban For. Urban Green.* **2018**, *34*, 85–96. [[CrossRef](#)]

44. Amani-beni, M.; Zhang, B.; Xie, G.; Xu, J. Impact of urban park's tree, grass and waterbody on microclimate in hot summer days: A case study of Olympic Park in Beijing, China. *Urban. For. Urban. Gree* **2018**, *32*, 1–6. [[CrossRef](#)]
45. Zhang, Z.; Lv, Y.; Pan, H. Cooling and humidifying effect of plant communities in subtropical urban parks. *Urban For. Urban Green* **2013**, *12*, 323–329. [[CrossRef](#)]
46. Gkatsopoulos, P. A Methodology for Calculating Cooling from Vegetation Evapotranspiration for Use in Urban Space Microclimate Simulations. *Procedia Environ. Sci.* **2017**, *38*, 477–484. [[CrossRef](#)]
47. Margaritis, E.; Kang, J.; Filipan, K.; Botteldooren, D. The influence of vegetation and surrounding traffic noise parameters on the sound environment of urban parks. *Appl. Geogr.* **2018**, *94*, 199–212. [[CrossRef](#)]
48. Wang, Y.F.; Ni, Z.B.; Wu, D.; Fan, C.; Lu, J.Q.; Xia, B.C. Factors influencing the concentration of negative air ions during the year in forests and urban green spaces of the Dapeng Peninsula in Shenzhen, China. *J. For. Res.* **2019**, *31*, 2537–2547. [[CrossRef](#)]
49. Cao, C.; Jiang, W.J.; Wang, B.Y.; Fang, J.H.; Lang, J.D.; Tian, G.; Jiang, J.; Zhu, T.F. Inhalable Microorganisms in Beijing's PM_{2.5} and PM₁₀ Pollutants during a Severe Smog Event. *Environ. Sci. Technol.* **2014**, *48*, 1499–1507. [[CrossRef](#)] [[PubMed](#)]
50. Chuang, M.T.; Chou, C.C.K.; Lin, N.H.; Takami, A.; Hsiao, T.C.; Lin, H.T.; Fu, J.S.; Pani, S.K.; Lu, Y.R.; Yang, T.Y. A Simulation Study on PM_{2.5} Sources and Meteorological Characteristics at the Northern Tip of Taiwan in the Early Stage of the Asian Haze Period. *Aerosol Air Qual. Res.* **2017**, *17*, 3166–3178. [[CrossRef](#)]
51. Wang, Y.; Zhuang, G.S.; Zhang, X.Y.; Huang, K.; Xu, C.; Tang, A.; Chen, J.M.; An, Z.S. The ion chemistry, seasonal cycle, and sources of PM_{2.5} and TSP aerosol in Shanghai. *Atmos. Environ.* **2006**, *40*, 2935–2952. [[CrossRef](#)]
52. Miao, S.; Zhang, X.Y.; Han, Y.J.; Sun, W.; Liu, C.J.; Yin, S. Random Forest Algorithm for the Relationship between Negative Air Ions and Environmental Factors in an Urban Park. *Atmosphere* **2018**, *9*, 463. [[CrossRef](#)]

Disclaimer/Publisher's Note: The statements, opinions and data contained in all publications are solely those of the individual author(s) and contributor(s) and not of MDPI and/or the editor(s). MDPI and/or the editor(s) disclaim responsibility for any injury to people or property resulting from any ideas, methods, instructions or products referred to in the content.